Published in final edited form as:
Microvasc Res. 2007 March ; 73(2): 84–94. doi:10.1016/j.mvr.2006.10.007.

Improved Growth Factor Directed Vascularization into Fibrin Constructs Through Inclusion of Additional Extracellular Molecules

JD Smith[†,§], **ME Melhem**[†], **KT Magge**[†], **AS Waggoner**[§], and **PG Campbell**[†,§,*]

[†] Institute for Complex Engineered Systems, Carnegie Mellon University, 5000 Forbes Ave., Pittsburgh, PA 15213

[§] Molecular Biosensor and Imaging Center Carnegie Mellon University, 4400 Fifth Ave., Pittsburgh, PA 15213

Abstract

Using the chick chorioallantoic membrane assay (CAM) and a novel histological technique we investigated the ability of blood vessels to directly invade fibrin-based scaffolds. In our initial experiments utilizing vascular endothelial growth factor ($VEGF_{165}$) we found no direct invasion. Instead, the fibrin was completely degraded and replaced with highly vascularized new tissue. Addition of fibroblast growth factor-2 (FGF-2), bone morphogenic protein-2 (BMP-2), or platelet-derived growth factor-BB (PDGF-BB) to the fibrin construct also did not result in construct vascularization. Because natural and regenerating tissues exhibit complex extracellular matrices (ECMs), we hypothesized that a more complex scaffold may improve blood vessel invasion. Addition of fibronectin, hyaluronic acid, and collagen type I within 20 mg/mL fibrin constructs resulted in no significant improvement. However, the same additive concentrations within 10 mg/mL fibrin constructs resulted in dramatic improvements, specifically with hyaluronic acid. Overall, we believe these results indicate the importance of structural and functional cues of not only in the initial scaffold but also as the construct is degraded and remodeled. Furthermore, the CAM assay may represent a useful model for understanding ECM interactions as well as for screening and designing tissue engineered scaffolds.

Keywords

extracellular matrix; angiogenesis; fibrin; histology; quantum dots

INTRODUCTION

Our laboratory uses the chick CAM assay to study blood vessel responses to fibrin-based constructs for use in designing bone tissue regeneration therapies. The chorioallantoic membrane (CAM) assay, used for more than half a century, has become a mainstay in the study of blood vessel development (Auerbach et al., 2003; Cruz et al., 2000; Cruz et al.,

[*]Correspondence should be addressed to: Phil Campbell, Ph.D., 1212 Hamburg Hall, Institute for Complex Engineered Systems, Carnegie Mellon University, 5000 Forbes Ave, Pittsburgh, PA, PA 15213, Phone: (412) 268-4126, Fax: (412) 268-5229, Email: pcampbel@cs.cmu.edu.

1997; DeFouw and DeFouw, 2000a; DeFouw and DeFouw, 2000b; Djonov et al., 2000a; Djonov et al., 2000b; McDonnell et al., 2005; Rizzo and DeFouw, 1996; Rizzo et al., 1995; Rizzo et al., 1993). The CAM assay has also proved useful for biological devices and in tissue engineering applications, particularly those concerning biocompatibility studies and angiogenic responses to tissue-engineered constructs (Borges et al., 2003a; Borges et al., 2003b; Nguyen et al., 1994; Ribatti et al., 2001; Rickert et al., 2003; Valdes et al., 2003; Valdes et al., 2002; Wong et al., 2003). In this work we extend the CAM assay in the development of a histological technique to specifically examine direct vascular invasion into fibrin-based constructs. Further, we used this technique to examine the effect of growth factor and scaffold composition on vascular invasion.

Visualization of CAM vascular ingrowth into the construct would ideally be performed *in situ*. To this end we have utilized intravitally injected quantum dots (QDs) to image the CAM blood vessel response to our fibrin-based constructs (submitted manuscript); however, the use of *in situ* fluorescence microscopy to examine vascularization of the construct proved to be inconclusive. Epifluorescence alone could not discriminate whether vessels were within the construct or residing underneath it. The fibrin itself became a highly scattering and optically dense material during the CAM response making *in vivo* analysis by optical sectioning techniques difficult. Additionally, micromovements of the CAM serve to further compound *in situ* imaging problems. Therefore, until we could develop improved *in situ* imaging techniques we decided to pursue a histological method.

Paraffin-based histology would provide conclusive evidence of fibrin vascularization, although this method is low throughput, laborious, and the process inherently induces artifacts. The ability to acquire timely results from a significant number of samples requires a technique that is both fast and robust. We developed a fast-analysis technique involving intravital injection of QDs, excision and fixation of the fibrin and connected CAM, and histological sectioning using a vibratome. We then applied this technique to study the effect of growth factors and fibrin composition on direct vascular invasion into the construct. The results of this study demonstrate a strong dependence of vascular response on scaffold composition, which we believe has significant implications for tissue engineering construct design.

METHODS

Fibrin Gel Formation

A solution was made containing human fibrinogen (gift of ZBL Behring, King of Prussia, PA), growth factor, and recombinant aprotinin (Sigma, St. Louis, MO) followed by incubation for 30 min at 37°C prior to gel formation to allow for growth factor-fibrinogen association. This solution was mixed with thrombin (Enzyme Research Labs, South Bend, IN) and transferred to 8 mm × 2 mm cylindrical molds to gel. Final concentrations in the gel were 20 mg/mL fibrinogen, 61.7 nM thrombin, 10 ng/mL growth factor, and 1 μg/mL aprotinin. Growth factors used include FGF-2 (PeproTech Inc., Rocky Hill, NJ), $VEGF_{165}$ (Chemicon, Temecula, CA), PDGF-BB (gift of Chiron, Emeryville, CA), and BMP-2 (R&D Systems, Minneapolis, MN). For experiments involving human fibronectin (Chemicon), fibronectin and Factor XIII (gift of ZBL Behring, King of Prussia, PA) were added to the fibrinogen solution at 100 μg/mL and 1 U/mL, respectively. Rooster comb hyaluronic acid (Sigma) was added to the fibrinogen solution as indicated. Vitrogen (PureCol) bovine collagen type I (Inamed, Fremont, CA) was neutralized according to the manufacturer's instructions and added to the fibrinogen solution just before gel formation. Gels containing collagen were allowed to gel for one hour before placement on the CAM.

Chick CAM Assay

White Leghorn eggs were purchased from a local farm and incubated at 38°C and 70% humidity in a rotating circulated air incubator (G.Q.F. Manufacturing Co., Savannah, GA). On day 3 eggs were cracked into Petri dishes containing 4 mL Dulbecco's Modified Eagles Medium (DMEM) (Gibco, Carslbad, CA) and incubated at 37°C. Fibrin constructs were placed on the CAM of 10-day old embryos.

Three days post-placement of the construct on the CAM 20–25 μL of amphiphilic 655 nm emitting quantum dots (QDs) (Quantum Dot Corp., Hayward, CA) (~ 15 nm in size) were injected into a large, easily accessible CAM vein using an aspirator tube assembly (Sigma) and borosilicate capillaries (Sutter Instruments, Novato, CA) pulled into micro-needles using a Model P-87 micropipette puller (Sutter Instruments). QD-labeled vessels were imaged *in situ* using an M2BIO stereomicroscope (Kramer Scientific, Valley Cottage, NY) with a 1.6X objective (0.075 NA), 0.6X zoom, Retiga Exi cooled CCD camera (QImaging, Burnaby, BC, Canada), QED InVivo imaging software v. 2.0.39 (Media Cybernetics, Siver Springs, MD), and an Ex:Em 460spuv:655/40 filter set (Chroma, Rockinghan, VT).

Histology and fluorescence imaging

After *in situ* imaging, the fibrin and surrounding CAM were excised and fixed in 1% glutaraldehyde and 3% paraformaldehyde (Electron Microscopy Sciences, Hatfield, PA) in PBS for 3 hours followed by three 5-min washes in PBS. Samples were sectioned perpendicularly in relation to their original orientation on the CAM at 300 μm thicknesses using a vibratome VT 1000S (Leica, Bannockburn, IL). Each resulting section was a cross-section containing the fibrin construct and underlying CAM. Sections were mounted on glass microslides including a coverslip and imaged for quantum dot (QD) fluorescence using a Zeiss Axioplan 2 (Thornwood, NY) epifluorescence microscope with a 2.5X objective (0.12NA), Zeiss AxioCam MRm CCD camera, and Zeiss AxioVision acquisition software v. 4.3. QDs with 655 nm emission were imaged using a Ex:Em 460spuv:655/40 filter set (Chroma) and a Zeiss AxioCam MRm CCD camera.

Transmission electron microscopy

Vibratomed sections of interest were washed with three changes of PBS followed by fixation with 1% OsO_4 buffered with PBS. After osmium fixation, sections were washed with three changes of dH_2O and dehydrated with an ascending series of EtOH (50%, 70%, 80%, 90% and 100%). Propylene oxide was used as a transitional solvent, and the specimens infiltrated with LR White (London Resin Company, Reading, Berkshire, England). The LR White was polymerized at 60°C for 48 hours. Thin (100nm) sections were cut using a diamond knife on a Reichert-Jung Ultracut E ultramicrotome (Leica, Wetzlar, Germany), picked up using copper grids, and stained with uranyl acetate, and lead citrate. The grids were viewed on a Hitachi H-7100 transmission electron microscope (Pleasanton, CA) operating at 50 kV. Digital images were obtained using an AMT Advantage 10 CCD Camera System (Advanced Microscopy Techniques Corporation, Danvers, MA) and NIH Image software (Bethesda, MD).

Scanning electron microscopy

Specimens were washed in 3 changes of PBS and fixed in 1% glutaraldehyde and 3% paraformaldehyde in PBS. After 3 washes of PBS, the specimens were fixed for one hour in 1% OsO_4 buffered with PBS. The OsO_4 was removed with 3 five-minute washes of dH_20, followed by dehydration in an ascending series of ethanol (50%, 70%, 80%, 90%, and 3 changes of 100%) The samples were held in each ethanol wash for 10 minutes and then held in 100% ethanol overnight. Samples were dried in a Pelco CPD2 critical point dryer (Clovis,

CA) using CO_2 at 1200 psi and 42°C. Dried specimens were attached to SEM stubs using double stick tape and coated with gold using a Pelco SC-6 sputter coater. Specimens were examined using a Hitachi 2460N Scanning Electron Microscope (Pleasanton, CA). Digital images were obtained using Quartz PCI Image software (Vancouver, BC, Canada).

RESULTS

Our laboratory is interested in directing cellular and tissue responses using immobilized growth factor patterns on and within fibrin-based constructs for use in basic discovery and bone tissue engineering applications (Campbell et al., 2005; Miller et al., 2006; Weiss et al., 2005). This approach is based on observations that growth factor spatial patterns are important for biological developmental as well as tissue regeneration and wound healing (Gerhardt et al., 2003; Ruhrberg et al., 2002; Singer and Clark, 1999; Tabata, 2001) and the idea that these patterns could be exploited to create improved therapies. In our first model studies we have been investigating CAM blood vessel ingrowth into fibrin constructs containing the simplest growth factor pattern, a uniform concentration of immobilized fibroblast growth factor-2 (FGF-2).

Because the fibrin became optically dense during the CAM response, determination of blood vessel ingrowth into these constructs was difficult to assess *in situ*. Therefore, we developed a novel histological technique to directly examine blood vessel invasion (Figure 1). Fibrin-based constructs were placed on chick CAMs (Figure 1A), and three days later CAM blood vessels were visualized via intravital injection of quantum dots (QDs) (Figure 1B). New blood vessels were seen forming a spoke-wheel pattern around the fibrin construct, and fluorescent structures, possibly blood vessels, were seen from what appeared to be within the construct.

The fibrin and connected CAM were excised, fixed in 1% glutaraldehyde and 3% paraformaldehyde, and then cut to 300 μm thick sections using a vibratome. Samples were mounted with the fibrin-CAM interface perpendicular to the cutting direction of the vibratome so that the invasive character of the CAM would be imaged in each section (Figure 1C). Contrary to what was inferred from Figure 1B, we determined that blood vessels did not directly invade the fibrin construct (Figure 1C). Instead, blood vessels developed only to the fibrin edge (Figure 1C). CAM tissue degraded the fibrin as a “front” and replaced it with “neo-tissue” full of new blood vessels, which followed closely behind the invasive front (manuscript in review). Vessels tended to be highly linear and were directed towards the construct (Figure 1C), most likely due to the chemotactic effect of FGF-2 as it was released from the degraded fibrin. Normally, the CAM is usually very thin and its blood vessels would reside solely in the plane perpendicular to the image in Figure 1C. Additionally, large-scale proliferation of the CAM tissue induced by the growth factor resulted in the umbrella shape of the fibrin, although contraction of the fibrin during the CAM response may also be a factor.

The inability of blood vessels to invade the fibrin prompted us to look for a way to improve direct vascular ingrowth into the fibrin construct. One possibility is the use of other angiogenic growth factors (Richardson et al., 2001; Wong et al., 2003). So, in addition to FGF-2, we individually tested platelet derived growth factor-BB (PDGF-BB), vascular endothelial growth factor ($VEGF_{165}$), and bone morphogenic protein-2 (BMP-2) at 1, 10, and 100 ng/mL, while keeping all other construct components constant. BMP-2 was included because it has been shown to induce a chick CAM angiogenic response ((Deckers et al., 2002; Raida et al., 2005); unpublished data) and because our interest lies in developing bone tissue engineering therapies. None of the growth factors at any of the concentrations tested improved fibrin vascularization, as evidenced by a clear distinction

between the fibrin (clear material in the brightfield images) and blood vessels and blood vessels (fluorescent structures) (Figure 2, data not shown). However, differences were qualitatively seen in the appearance of the responding blood vessels as well as the "thickness" of the CAM invasive zone at the fibrin edge.

Interestingly, PDGF-BB was the only growth factor that consistently induced lobes of cellular invasion ahead of the main CAM/fibrin interface (Figure 3), although these lobes were not vascularized. These lobes were further analyzed by transmission electron microscopy (TEM) (Figure 3B, C). That vibratomed sections of interest can also be further processed using more traditional histological analysis such as immunohistochemistry or TEM is a key advantage of our technique. Fibrin at the lobe edge (boxed area of Figure 3A) had large pores due to local degradation whereas fibrin farther from the lobe appeared more homogeneous (Figure 3B), an indication of cell-mediated fibrin degradation. Cells of a phagocytic nature appear to predominate at the lobe front (Figure 3C) although their identity has yet to be verified. As a side note, QD fluorescence does not survive osmium treatment but can be identified physically as electron dense particles in TEM images (submitted manuscript).

Because these growth factors did not improve vascularization we took another approach, re-formulation of the construct. ECMs formed during wound healing or tissue regeneration are complex and evolving structures, with each molecular species providing chemical and/or mechanical cues (Clark, 1985; Clark, 1993b). Therefore, a lack of vascularization may be due to a lack of ECM complexity. To test this we incorporated 0.1 mg/mL fibronectin, 1.5 mg/mL hyaluronic acid, or 1.2 mg/mL collagen type I into 20 mg/mL fibrin constructs containing 10 ng/mL $VEGF_{165}$. These molecules are early/mid-, mid-, and late-stage ECM molecules, respectively and are found in the granulation tissue of the wound healing process (Clark, 1985; Clark, 1993b; Gailit and Clark, 1994). Concentrations of these components within the fibrin constructs were chosen based on formulation constraints.

Examination of these initial construct variations 3 days post-placement on the CAM showed no significant improvement (Figure 4). Fibronectin-containing constructs induced cellular invasive "fingers". However, these fingers were not vascularized, nor was an improvement found in overall direct vascular invasion (Figure 4C, D). Fibrin containing 1.2 mg/mL bovine collagen type I also did not exhibit improved vascularization but did show diffuse cellular invasion ahead of the fibrin-CAM boundary (data not shown). Although addition of the ECM components resulted in small changes, significant improvement on direct vascularization of the construct did not occur.

We next examined the effect of these additives within constructs of lower fibrin density (10 mg/mL). As before, these constructs were examined three days post-placement on the CAM. Significant improvements over their 20 mg/mL counterparts (Figure 5) were seen. Interestingly, fibrin-only constructs now exhibited cellular invasive fingers similar to that of fibronectin-containing constructs at both 10 mg/mL and 20 mg/mL fibrin (Figure 4C, D; Figure 5A–D). Fibronectin-containing constructs also demonstrated the umbrella shape characteristic of the fibrin-only construct (Figure 5C–F vs. Figure 5A, B).

In contrast, collagen-fibrin constructs demonstrated a significantly different response. The construct was evenly contacted by the CAM and no longer exhibited the characteristic umbrella shape (Figure 5G, H). New vessels were not localized to the center, and a high concentration of small vessels appeared to make intimate contact with the construct, possibly even demonstrating slight fibrin invasion (Figure 5H). H&E staining showed individual, non-vascular associated fibroblast-like cells throughout the entire construct (data not shown).

Hyaluronic acid had the most dramatic affect on the CAM response. Various shaded regions within the fibrin showed that there was significant remodeling of the entire construct during the CAM response (Figure 5I). Significant blood vessel invasion also appeared to have occurred (Figure 5J). These constructs adhered strongly to the CAM. In fact, they integrated so well that the CAM sometimes grew over the top of the material, which is why blood vessels were seen on all sides of the construct (Figure 5J asterisks).

Cellular and vascular responses to ECM additives shown in Figure 5 were semi-quantitated by rating on a 1 to 4 basis (Table 1). Extent of construct remodeling and cellular invasion correlated, which was to be expected. Interestingly, the data also indicates that the sheer number, or density, of responding vessels within the CAM does not translate to vascular invasion.

ECM additives can affect construct architecture, and these alterations may influence the differential responses that were observed. Therefore, we examined the construct architecture using scanning electron microscopy (SEM). Both 10 mg/mL and 20 mg/mL fibrin gels containing ECM additives at the same concentrations tested earlier were prepared and analyzed by SEM (Figure 6). Observation of structure typically required sample cross-sections, which sometimes resulted in induced artifacts. These artifacts were seen as plate-like and solid structures in the images (Figure 6B, E, F asterisks).

As expected fibrin fibril packing was more dense at 20 mg/mL than at 10 mg/mL. Construct architecture was essentially unchanged with the addition of fibronectin (Figure 6A, E vs. Figure 6B, F). Collagen induced the formation of small ~ 1 μm sized pores at 10 mg/mL fibrin, which became more defined at 20 mg/mL (Figure 6C, G). As reported in the literature hyaluronic acid altered the fibrin structure (LeBoeuf et al., 1987; Weigel et al., 1986). It induced a bimodal architecture forming large “struts” of tightly packed, highly parallel fibrin fibrils, which resulted in a more open architecture (Figure 6D, H).

We quantified fibril and strut diameters in the Figure 6 images, revealing that all constructs are composed of ~ 30 nm thick fibrils (Table 2). At 10 mg/mL fibrin hyaluronic acid induced approximately 3-fold smaller struts than at 20 mg/mL. Overall, structures at 10 mg/mL fibrin were not drastically different than structures at 20 mg/mL although collagen and hyaluronic acid-containing constructs were significantly different than those of fibrin-only and fibrin-fibronectin constructs.

DISCUSSION

In this work we have described the development and implementation of a new histological method for investigating vascularization of constructs in the chick CAM assay. This technique has multiple advantages. The backbone of this technique is the extreme brightness of QDs and their ability to survive fixation (submitted manuscript). We typically fix our samples for 3 hours but overnight fixation is also possible. In addition, the vibratoming process is less intrusive to the sample; no harsh chemical treatments are performed and the thicker sections mean less sample cutting is involved. Thick vibratome sections also provide three-dimensional information that could not be easily obtained with ~ 5 μm sectioned paraffin-processed samples. This technique is also fast; the time between injection of QDs and imaging of vibratomed sections (as seen in Figure 1) can be as little as 4–5 hours. Additionally, our technique also allows sections to be analyzed further by paraffin-based histological analysis or TEM analysis (Figure 3, submitted manuscript).

The histological method presented in this work is not without some difficulties. The CAM does not cut easily with the vibratome, which can sometimes result in rips or separation from the fibrin (see Figure 4D, E). Samples are mounted to a plate with their CAM/fibrin

interface perpendicular to the blade. Those samples that are wide but not thick can be somewhat floppy and typically section poorly. We have experimented with embedding samples in blocks of fibrin, gelatin, and agar. The CAM does not adhere well to any of these materials, and the sample eventually works its way free of the embedding material during cutting (data not shown). Solutions to this problem are still being investigated. Additionally, we are investigating the possibility of cryosectioning our samples which will completely remove these issues. However, it should be stressed that the current assay is still quite easy to perform and samples are typically processed with a high success rate.

Another difficulty is presented in Figure 5 (Figure 5J, K, L), where the interface between the invading CAM and the fibrin is not distinctive. Although blood vessels appear to invade fibrin containing hyaluronic acid, fluorescent labeling of the fibrin will be needed to confirm this. We are investigating biotinylation of fibrinogen followed by binding by streptavidin-QDs. Initial work using this technique has produced positive results in delineating blood vessel and fibrin localization (Accepted manuscript for Microvascular Research).

Embryo deaths were not completely uncommon during the course of these experiments, something which is common for any CAM assay experiment. Although healthy 10-day old embryos had a high survival rate compared to freshly cracked eggs. Embryo health can also produce variability in CAM responses. Therefore, extreme care was taken to not only use the healthiest embryos (with intact yolk sacs) but also to incorporate a higher number of sample duplicates to ensure reproducibility.

Unlike the addition of growth factors, changes in the construct composition had dramatic effects on the CAM vascular response. These effects may be due, in part, to the inherent characteristics of the additive ECM, the action of growth factors in concert with ECM molecules, changes to overall fibrin architecture, and ECM molecule concentration.

Fibronectin is a large dimeric protein that is found in early to mid stages of wound healing ECMs and it contains numerous cell- and ECM protein-binding moieties (Gailit and Clark, 1994; Magnusson and Mosher, 1998; Miyamoto et al., 1998; Potts and Campbell, 1996). Additionally, fibronectin can act as a depot for some growth factors (Gailit and Clark, 1994). Interestingly, initial TEM analysis of fibronectin-containing samples revealed a unique cell-type at the forefront of the cellular “fingers,” reminiscent of the cells seen in Figure 3. Monocytes and macrophages have been shown to lead invasion into matrigel constructs in mice (Anghelina et al., 2004). To this end the presence of monocytes and macrophages as the lead invasive cell-type is currently under investigation.

Collagen type I, a late stage ECM protein in wound healing, forms the majority of the final ECM of most tissues (Miller and Gay, 1987; Yang et al., 2004). Collagen is known to produce proliferative and functional responses through cell binding and signaling (Lin and Bissell, 1993; Weinberg and Bell, 1985). Collagen and collagen-derived peptides have also been shown to be chemoattractants for fibroblasts *in vitro* (Postlethwaite et al., 1978). This correlates with our results in the 10 mg/mL fibrin-1.2mg/mL collagen type I case, where fibroblast-like cells were seen in H&E stained sections (data not shown).

Hyaluronic acid, although not a protein, is an essential component of wound healing ECMs (Clark, 1985; Clark, 1993a; Savanni and Bagli, 2000; Weigel et al., 1986). Hyaluronic acid directly affects fibrin polymerization, causing the gel to swell and become more porous (Hayen et al., 1999; LeBoeuf et al., 1987; LeBoeuf et al., 1986; Weigel et al., 1989; Weigel et al., 1986). Cell migration is also stimulated by hyaluronic acid (Chen and Abatangelo, 1999; Weigel et al., 1986). High molecular weight hyaluronic acid is antiangiogenic but, similar to fibrin, hyaluronic acid’s degradation products are angiogenic (West et al., 1985).

Cells interact with ECM molecules using integrins and cell-surface receptors (Gailit and Clark, 1994). Fibrin, fibronectin, and collagen are all bound by specific integrins while hyaluronic acid is bound by three classes of non-integrin surface receptors (Chen and Abatangelo, 1999). Integrin-ligand binding can lead to cytoskeletal reorganization, intracellular signaling, and gene expression (Bissell et al., 1982; Geiger et al., 2001). As a result, specific integrin-ligand interactions may result in differential cellular responses. Additionally, different cell types differentially express specific integrins, therefore their responses to ECM proteins would be expected to vary from cell to cell.

Modulation of growth factor action is another possible reason for the differences in vascular responses seen in these studies. Growth factor receptor-integrin interactions have been shown to modulate cellular responses to growth factors (Borges et al., 2000; Doerr and Jones, 1996; Guo et al., 2001; Jikko et al., 1999). Therefore, unique ECM compositions may modulate cellular responses to the same growth factor. One reason for this modulation may be that both integrin and growth factor signaling utilize many of the same intracellular proteins (Borges et al., 2000). This interaction may also arise from the bridging of growth factor receptors and integrins via ECM molecules that contain integrin binding sites and bound growth factor (Fontana et al., 2005). Involvement of lipid rafts have been implicated, although this idea is still somewhat controversial (Decker et al., 2004).

The concentrations of ECM additives also played a significant role in the CAM blood vessel response. The concentrations tested represent the upper limit that could be achieved while keeping the fibrin at 20 mg/mL. Fibronectin concentrations were especially low due to low stock concentrations. However, at 10 mg/mL fibrin, 0.6 mg/mL fibronectin was tested. This concentration resulted in stronger cellular invasion than at 0.1 mg/mL, but it still lacked direct vascular invasion (data not shown). Lower concentrations of collagen type I and hyaluronic acid were tested. As expected, CAM vessel responses approached the fibrin-only case as ECM additive concentrations were lowered (data not shown).

Fibrin concentration demonstrated a unique role in the range of CAM vascular responses seen. Construct structure was not significantly different at 10 mg/mL vs. 20 mg/mL for all constructs tested (Figure 6). However, CAM vascular responses were very different (Figure 4, 5). Therefore, it would seem that 20 mg/mL fibrin “masked” the signalling function of collagen and hyaluronic acid. Additionally, cellular invasive “fingers” seen with 10 mg/mL fibrin only, as compared to the lack of invasion at 20 mg/mL, would indicate an inhibitory effect of high fibrin concentrations. Overall, for only a two-fold change in fibrin density, construct remodeling, degradation, and vascular responses were dramatically different. The reason for this dominant effect of fibrin most likely represents an amalgamation of all the factors mentioned above.

Prior studies have reported vascularizaton of tissue engineered constructs using both synthetic and naturally-derived constructs containing growth factors and/or cells (for examples see (Borges et al., 2003a; Borges et al., 2003b; Elcin and Elcin, 2006; Ganta et al., 2003; Kaigler et al., 2006; Murphy et al., 2004; Tanihara et al., 2001; Yao et al., 2004; Zisch et al., 2003)). However, the primary focus of these studies did not address the manner of directed vascular invasion into the matrix, but only upon the end extent of vacularization. Our work is different from these prior studies in that we are not only interested in directing vascularization into our constructs, but also in understanding the process of directed vascular invasion.

The histological method we have demonstrated allows for the determination of directed angiogenesis into fibrin-based constructs. Other similar techniques also exist. Brey et al. developed a technique to determine vascular invasion into fibrin constructs where three-

dimensional reconstructions of vasculature within implanted constructs were obtained from alignment and stacking of individually immunostained cryosections (Brey et al., 2002). This technique is very powerful but suffers from low-throughput as well as sectioning and staining artifacts. We are currently developing optical sectioning techniques to couple with our histological method to hopefully achieve comparable three-dimensional reconstructions but with less sample manipulation and more rapid turnaround.

Another innovative technique is that developed by Guedez et al. where ECM-filled semiclosed silicon cylinders are implanted subcutaneously in rats and directed vascular ingrowth into the silicon tube was visualized and quantitated using fluorescein-based fluorescent dyes (Guedez et al., 2003). This technique is quantitative but requires the use of silicon tubing implantation, which is not amenable to the CAM assay. We believe that our histological method, coupled with our development of quantum dot technology, incorporates many of the positive aspects of these techniques but improves on versatility and processing speed.

These results of this work show the power of the chick CAM assay as an *in vivo* model. The rapid experimental time, the inexpensive nature of the CAM assay, and the histological technique we developed allow for an *in vivo* model capable of comparing a large number of constructs that may not be possible in more expensive animal models. Using the CAM assay in this manner we have clearly demonstrated the importance of scaffold design on vascular responses. The question now lies in the ability of the CAM assay to translate into mammalian models that may then have relevance to clinical application to humans. These experiments are currently underway in our laboratory. If the CAM assay is translatable, then it could provide a powerful screening system with which to develop optimal scaffolds for further examination in more expensive and time-consuming mammalian models.

Supplementary Material

Refer to Web version on PubMed Central for supplementary material.

Acknowledgments

The authors would like to thank the National Science Foundation (CTS-0210238), National Institutes of Health (1 R01 EB00 364-01 and 1 T32 EB00424-03), and Pennsylvania Infrastructure and Technology Alliance for their support of this work. We would also like to thank Joe Suhan at Carnegie Mellon for his SEM and TEM work, and Quantum Dot Corporation (Marcel Bruchez, Hayward, CA) for their generous gift of quantum dots.

Bibliography

Anghelina M, Krishnan P, Moldovan L, Moldovan NI. Monocytes and macrophages form branched cell columns in matrigel: implications for a role in neovascularization. Stem Cells Dev 2004;13:665–76. [PubMed: 15684834]

Auerbach R, Lewis R, Shinners B, Kubai L, Akhtar N. Angiogenesis assays: a critical overview. Clin Chem 2003;49:32–40. [PubMed: 12507958]

Bissell MJ, Hall HG, Parry G. How does the extracellular matrix direct gene expression? J Theor Biol 1982;99:31–68. [PubMed: 6892044]

Borges E, Jan Y, Ruoslahti E. Platelet-derived growth factor receptor beta and vascular endothelial growth factor receptor 2 bind to the beta 3 integrin through its extracellular domain. J Biol Chem 2000;275:39867–73. [PubMed: 10964931]

Borges J, Mueller MC, Padron NT, Tegtmeier F, Lang EM, Stark GB. Engineered adipose tissue supplied by functional microvessels. Tissue Eng 2003a;9:1263–70. [PubMed: 14670114]

Borges J, Tegtmeier FT, Padron NT, Mueller MC, Lang EM, Stark GB. Chorioallantoic membrane angiogenesis model for tissue engineering: a new twist on a classic model. Tissue Eng 2003b; 9:441–50. [PubMed: 12857412]

Brey EM, King TW, Johnston C, McIntire LV, Reece GP, Patrick CW Jr. A technique for quantitative three-dimensional analysis of microvascular structure. Microvasc Res 2002;63:279–94. [PubMed: 11969305]

Campbell PG, Miller ED, Fisher GW, Walker LM, Weiss LE. Engineered spatial patterns of FGF-2 immobilized on fibrin direct cell organization. Biomaterials 2005;26:6762–70. [PubMed: 15941581]

Chen WY, Abatangelo G. Functions of hyaluronan in wound repair. Wound Repair Regen 1999;7:79–89. [PubMed: 10231509]

Clark RA. Cutaneous tissue repair: basic biologic considerations. I J Am Acad Dermatol 1985;13:701–25.

Clark RA. Basics of cutaneous wound repair. J Dermatol Surg Oncol 1993a;19:693–706. [PubMed: 8349909]

Clark RA. Biology of dermal wound repair. Dermatol Clin 1993b;11:647–66. [PubMed: 8222349]

Cruz A, DeFouw LM, DeFouw DO. Restrictive endothelial barrier function during normal angiogenesis in vivo: partial dependence on tyrosine dephosphorylation of beta-catenin. Microvasc Res 2000;59:195–203. [PubMed: 10684725]

Cruz A, Rizzo V, De Fouw DO. Microvessels of the chick chorioallantoic membrane uniformly restrict albumin extravasation during angiogenesis and endothelial cytodifferentiation. Tissue Cell 1997;29:277–81. [PubMed: 9225483]

Decker L, Baron W, Ffrench-Constant C. Lipid rafts: microenvironments for integrin-growth factor interactions in neural development. Biochem Soc Trans 2004;32:426–30. [PubMed: 15157152]

Deckers MM, van Bezooijen RL, van der Horst G, Hoogendam J, van Der Bent C, Papapoulos SE, Lowik CW. Bone morphogenetic proteins stimulate angiogenesis through osteoblast-derived vascular endothelial growth factor A. Endocrinology 2002;143:1545–53. [PubMed: 11897714]

DeFouw LM, DeFouw DO. Differentiation of endothelial barrier function during normal angiogenesis requires homotypic VE-cadherin adhesion. Tissue Cell 2000a;32:238–42. [PubMed: 11037794]

DeFouw LM, DeFouw DO. Vascular endothelial growth factor fails to acutely modulate endothelial permeability during early angiogenesis in the chick chorioallantoic membrane. Microvasc Res 2000b;60:212–21. [PubMed: 11078637]

Djonov V, Schmid M, Tschanz SA, Burri PH. Intussusceptive angiogenesis: its role in embryonic vascular network formation. Circ Res 2000a;86:286–92. [PubMed: 10679480]

Djonov VG, Galli AB, Burri PH. Intussusceptive arborization contributes to vascular tree formation in the chick chorio-allantoic membrane. Anat Embryol (Berl) 2000b;202:347–57. [PubMed: 11089926]

Doerr ME, Jones JI. The roles of integrins and extracellular matrix proteins in the insulin-like growth factor I-stimulated chemotaxis of human breast cancer cells. J Biol Chem 1996;271:2443–7. [PubMed: 8576205]

Elcin AE, Elcin YM. Localized angiogenesis induced by human vascular endothelial growth factor-activated PLGA sponge. Tissue Eng 2006;12:959–68. [PubMed: 16674307]

Fontana L, Chen Y, Prijatelj P, Sakai T, Fassler R, Sakai LY, Rifkin DB. Fibronectin is required for integrin alphavbeta6-mediated activation of latent TGF-beta complexes containing LTBP-1. Faseb J 2005;19:1798–808. [PubMed: 16260650]

Gailit J, Clark RA. Wound repair in the context of extracellular matrix. Curr Opin Cell Biol 1994;6:717–25. [PubMed: 7530463]

Ganta SR, Piesco NP, Long P, Gassner R, Motta LF, Papworth GD, Stolz DB, Watkins SC, Agarwal S. Vascularization and tissue infiltration of a biodegradable polyurethane matrix. J Biomed Mater Res A 2003;64:242–8. [PubMed: 12522810]

Geiger B, Bershadsky A, Pankov R, Yamada KM. Transmembrane crosstalk between the extracellular matrix--cytoskeleton crosstalk. Nat Rev Mol Cell Biol 2001;2:793–805. [PubMed: 11715046]

Gerhardt H, Golding M, Fruttiger M, Ruhrberg C, Lundkvist A, Abramsson A, Jeltsch M, Mitchell C, Alitalo K, Shima D, et al. VEGF guides angiogenic sprouting utilizing endothelial tip cell filopodia. J Cell Biol 2003;161:1163–77. [PubMed: 12810700]

Guedez L, Rivera AM, Salloum R, Miller ML, Diegmueller JJ, Bungay PM, Stetler-Stevenson WG. Quantitative assessment of angiogenic responses by the directed in vivo angiogenesis assay. Am J Pathol 2003;162:1431–9. [PubMed: 12707026]

Guo P, Xu L, Pan S, Brekken RA, Yang ST, Whitaker GB, Nagane M, Thorpe PE, Rosenbaum JS, Su Huang HJ, et al. Vascular endothelial growth factor isoforms display distinct activities in promoting tumor angiogenesis at different anatomic sites. Cancer Res 2001;61:8569–77. [PubMed: 11731444]

Hayen W, Goebeler M, Kumar S, Riessen R, Nehls V. Hyaluronan stimulates tumor cell migration by modulating the fibrin fiber architecture. J Cell Sci 1999;112 (Pt 13):2241–51. [PubMed: 10362554]

Jikko A, Harris SE, Chen D, Mendrick DL, Damsky CH. Collagen integrin receptors regulate early osteoblast differentiation induced by BMP-2. J Bone Miner Res 1999;14:1075–83. [PubMed: 10404007]

Kaigler D, Wang Z, Horger K, Mooney DJ, Krebsbach PH. VEGF scaffolds enhance angiogenesis and bone regeneration in irradiated osseous defects. J Bone Miner Res 2006;21:735–44. [PubMed: 16734388]

LeBoeuf RD, Gregg RR, Weigel PH, Fuller GM. Effects of hyaluronic acid and other glycosaminoglycans on fibrin polymer formation. Biochemistry 1987;26:6052–7. [PubMed: 3689758]

LeBoeuf RD, Raja RH, Fuller GM, Weigel PH. Human fibrinogen specifically binds hyaluronic acid. J Biol Chem 1986;261:12586–92. [PubMed: 3745204]

Lin CQ, Bissell MJ. Multi-faceted regulation of cell differentiation by extracellular matrix. Faseb J 1993;7:737–43. [PubMed: 8330681]

Magnusson MK, Mosher DF. Fibronectin: structure, assembly, and cardiovascular implications. Arterioscler Thromb Vasc Biol 1998;18:1363–70. [PubMed: 9743223]

McDonnell K, Bowden ET, Cabal-Manzano R, Hoxter B, Riegel AT, Wellstein A. Vascular leakage in chick embryos after expression of a secreted binding protein for fibroblast growth factors. Lab Invest 2005;85:747–55. [PubMed: 15806140]

Miller ED, Fisher GW, Weiss LE, Walker LM, Campbell PG. Dose-dependent cell growth in response to concentration modulated patterns of FGF-2 printed on fibrin. Biomaterials 2006;27:2213–21. [PubMed: 16325254]

Miller EJ, Gay S. The collagens: an overview and update. Methods Enzymol 1987;144:3–41. [PubMed: 3306286]

Miyamoto S, Katz BZ, Lafrenie RM, Yamada KM. Fibronectin and integrins in cell adhesion, signaling, and morphogenesis. Ann N Y Acad Sci 1998;857:119–29. [PubMed: 9917837]

Murphy WL, Simmons CA, Kaigler D, Mooney DJ. Bone regeneration via a mineral substrate and induced angiogenesis. J Dent Res 2004;83:204–10. [PubMed: 14981120]

Nguyen M, Shing Y, Folkman J. Quantitation of angiogenesis and antiangiogenesis in the chick embryo chorioallantoic membrane. Microvasc Res 1994;47:31–40. [PubMed: 7517489]

Postlethwaite AE, Seyer JM, Kang AH. Chemotactic attraction of human fibroblasts to type I, II, and III collagens and collagen-derived peptides. Proc Natl Acad Sci U S A 1978;75:871–5. [PubMed: 204938]

Potts JR, Campbell ID. Structure and function of fibronectin modules. Matrix Biol 1996;15:313–20. discussion 321. [PubMed: 8981327]

Raida M, Clement JH, Leek RD, Ameri K, Bicknell R, Niederwieser D, Harris AL. Bone morphogenetic protein 2 (BMP-2) and induction of tumor angiogenesis. J Cancer Res Clin Oncol 2005;131:741–50. [PubMed: 16136355]

Ribatti D, Nico B, Vacca A, Roncali L, Burri PH, Djonov V. Chorioallantoic membrane capillary bed: a useful target for studying angiogenesis and anti-angiogenesis in vivo. Anat Rec 2001;264:317–24. [PubMed: 11745087]

Richardson TP, Peters MC, Ennett AB, Mooney DJ. Polymeric system for dual growth factor delivery. Nat Biotechnol 2001;19:1029–34. [PubMed: 11689847]

Rickert D, Moses MA, Lendlein A, Kelch S, Franke RP. The importance of angiogenesis in the interaction between polymeric biomaterials and surrounding tissue. Clin Hemorheol Microcirc 2003;28:175–81. [PubMed: 12775899]

Rizzo V, DeFouw DO. Capillary sprouts restrict macromolecular extravasation during normal angiogenesis in the chick chorioallantoic membrane. Microvasc Res 1996;52:47–57. [PubMed: 8812754]

Rizzo V, Kim D, Duran WN, DeFouw DO. Ontogeny of microvascular permeability to macromolecules in the chick chorioallantoic membrane during normal angiogenesis. Microvasc Res 1995;49:49–63. [PubMed: 7538192]

Rizzo V, Steinfeld R, Kyriakides C, DeFouw DO. The microvascular unit of the 6-day chick chorioallantoic membrane: a fluorescent confocal microscopic and ultrastructural morphometric analysis of endothelial permselectivity. Microvasc Res 1993;46:320–32. [PubMed: 8121316]

Ruhrberg C, Gerhardt H, Golding M, Watson R, Ioannidou S, Fujisawa H, Betsholtz C, Shima DT. Spatially restricted patterning cues provided by heparin-binding VEGF-A control blood vessel branching morphogenesis. Genes Dev 2002;16:2684–98. [PubMed: 12381667]

Savanni, RC.; Bagli, DJ. The Role of Hyaluronan - Receptor Interactions in Wound Repair. In: Garg, HG., editor. Scarless Wound Healing. Marcel Dekker Incorporated; New York: 2000. p. 115-142.

Singer AJ, Clark RA. Cutaneous wound healing. N Engl J Med 1999;341:738–46. [PubMed: 10471461]

Tabata T. Genetics of morphogen gradients. Nat Rev Genet 2001;2:620–30. [PubMed: 11483986]

Tanihara M, Suzuki Y, Yamamoto E, Noguchi A, Mizushima Y. Sustained release of basic fibroblast growth factor and angiogenesis in a novel covalently crosslinked gel of heparin and alginate. J Biomed Mater Res 2001;56:216–21. [PubMed: 11340591]

Valdes TI, Klueh U, Kreutzer D, Moussy F. Ex ova chick chorioallantoic membrane as a novel in vivo model for testing biosensors. J Biomed Mater Res A 2003;67:215–23. [PubMed: 14517879]

Valdes TI, Kreutzer D, Moussy F. The chick chorioallantoic membrane as a novel in vivo model for the testing of biomaterials. J Biomed Mater Res 2002;62:273–82. [PubMed: 12209948]

Weigel PH, Frost SJ, LeBoeuf RD, McGary CT. The specific interaction between fibrin(ogen) and hyaluronan: possible consequences in haemostasis, inflammation and wound healing. Ciba Found Symp 1989;143:248–61. discussion 261–4, 281–5. [PubMed: 2680346]

Weigel PH, Fuller GM, LeBoeuf RD. A model for the role of hyaluronic acid and fibrin in the early events during the inflammatory response and wound healing. J Theor Biol 1986;119:219–34. [PubMed: 3736072]

Weinberg CB, Bell E. Regulation of proliferation of bovine aortic endothelial cells, smooth muscle cells, and adventitial fibroblasts in collagen lattices. J Cell Physiol 1985;122:410–4. [PubMed: 3881465]

Weiss LE, Amon CH, Finger S, Miller ED, Romero D, Verdinelli I, Walker LM, Campbell PG. Bayesian computer-aided experimental design of heterogenous scaffolds for tissue engineering. Computer-Aided Design 2005;37:1127–1139.

West DC, Hampson IN, Arnold F, Kumar S. Angiogenesis induced by degradation products of hyaluronic acid. Science 1985;228:1324–6. [PubMed: 2408340]

Wong C, Inman E, Spaethe R, Helgerson S. Fibrin-based biomaterials to deliver human growth factors. Thromb Haemost 2003;89:573–82. [PubMed: 12624643]

Yang C, Hillas PJ, Baez JA, Nokelainen M, Balan J, Tang J, Spiro R, Polarek JW. The application of recombinant human collagen in tissue engineering. BioDrugs 2004;18:103–19. [PubMed: 15046526]

Yao C, Prevel P, Koch S, Schenck P, Noah EM, Pallua N, Steffens G. Modification of collagen matrices for enhancing angiogenesis. Cells Tissues Organs 2004;178:189–96. [PubMed: 15812146]

Zisch AH, Lutolf MP, Ehrbar M, Raeber GP, Rizzi SC, Davies N, Schmokel H, Bezuidenhout D, Djonov V, Zilla P, et al. Cell-demanded release of VEGF from synthetic, biointeractive cell ingrowth matrices for vascularized tissue growth. Faseb J 2003;17:2260–2. [PubMed: 14563693]

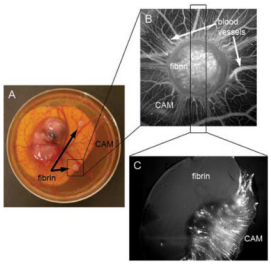

Figure 1. Histological assay to determine direct vascular invasion into fibrin

A. 20 mg/mL fibrin gels containing 10 ng/mL FGF-2 were placed on the CAM of 10 day old embryos (12 day old embryo is shown in panel A). B. Three days post-placement on the CAM, fluorescent QDs were intravitally injected and the blood vessels were imaged by fluorescence on an M2BIO stereoscope. C. The fibrin and connected CAM were excised and fixed in 1% paraformaldehyde and 3% glutaraldehyde in PBS for 3 hours followed by 3 washes in PBS. Samples were vibratomed perpendicularly to the CAM at 300 μm thickness. The fluorescence of the section shows that blood vessels form up to the fibrin edge but do not directly invade the fibrin.

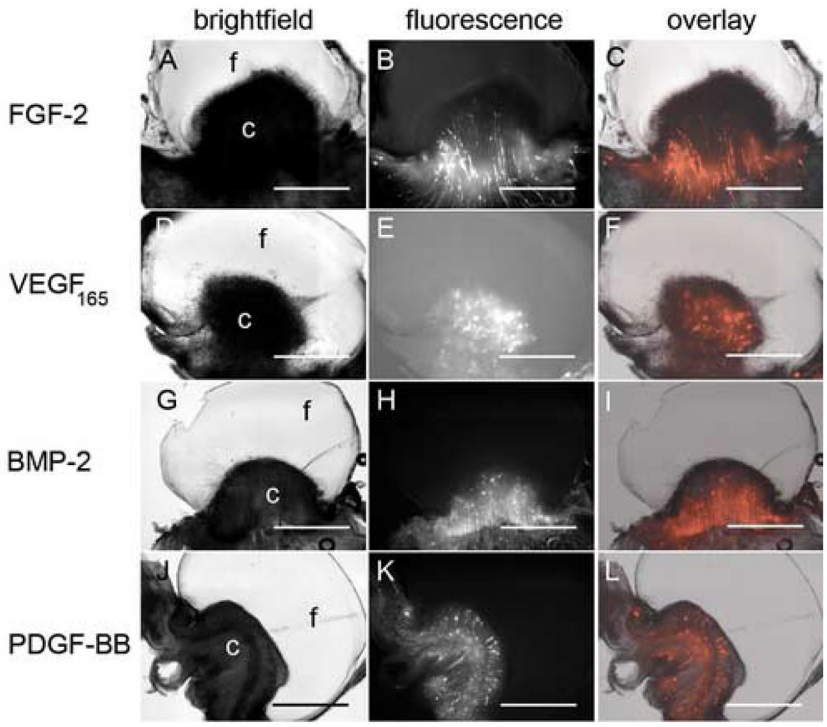

Figure 2. Fibrin 2. Growth factor choice does not improve fibrin vascularization

20 mg/mL fibrin gels containing 10 ng/mL FGF-2 (A–C), $VEGF_{165}$ (D–F), BMP-2 (G–I), and PDGF-BB (J–L) were placed on CAM of 10 day old chick embryos. Three days post-placement on the CAM, embryos were intravitally injected with QDs and histologically processed as in Figure 1. Brightfield (A, D, G, J) and fluorescence (B, E, H, K) images were obtained using the M2BIO stereoscope. Fluorescence overlays (C, F, I, L) are shown for comparison of blood vessel and fibrin localization. In panels A, D, G, and J “f” and “c” indicate the location of the fibrin and CAM, respectively. Scale bars in all images are 200 μm.

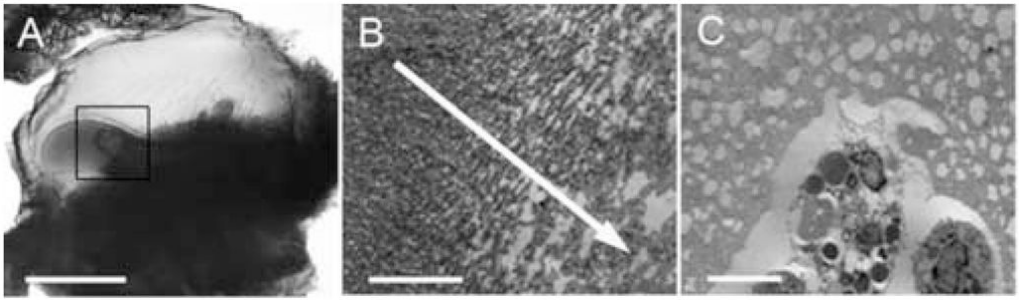

Figure 3. TEM analysis of fibrin containing PDGF-BB

20 mg/mL fibrin containing 10 ng/mL PDGF-BB was placed on the CAM of 10 day old chick embryos. Three days post-placement on the CAM, embryos were intravitally injected with QDs and histologically processed as in Figure 1. A. Brightfield image of a histological section showing lobes of cellular invasion. B. The section from panel A was processed for TEM analysis. The TEM image from the region of the boxed area in panel A shows the fibrin structure. The arrow leads towards the area of cellular invasive as evidenced by the increasing pore size caused by fibrin degradation. C. TEM image of phagocytic cell-types invading the partially degraded fibrin area at the forefront of the lobe of cellular invasion shown in panel A. Scale bars in A, B, and C are 200, 5, and 5 μm, respectively.

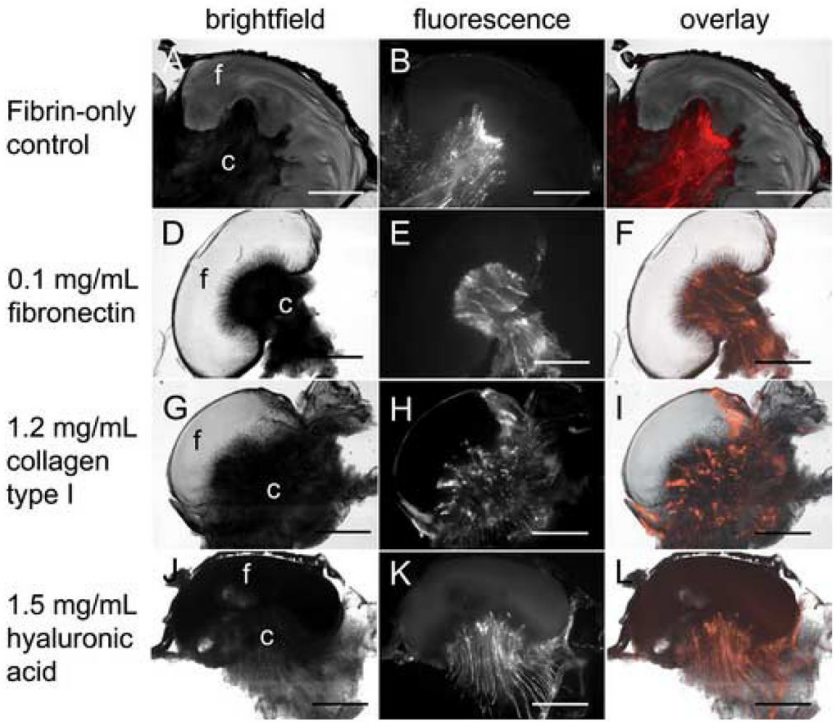

Figure 4. ECM additives within 20 mg/mL fibrin do not significantly improve vascularization

20 mg/mL fibrin gels containing 10 ng/mL $VEGF_{165}$ (A–C) or $VEGF_{165}$ and 0.1 mg/mL human fibronectin (D–F), 1.2 mg/mL bovine collagen type I (G–I), or 1.5 mg/mL rooster comb hyaluronic acid (J–L) were placed on the CAM of 10 day old chick embryos. Three days post-placement on the CAM, embryos were intravitally injected with QDs and histologically processed as in Figure 1. Brightfield (A, D, G, J) and fluorescence (B, E, H, K) images were obtained using the M2BIO stereoscope. Fluorescence overlays (C, F, I, L) are shown for comparison of blood vessel and fibrin localization. In panels A, D, G, and J "f" and "c" indicate the location of the fibrin and CAM, respectively. Scale bars in all images are 200 μm.

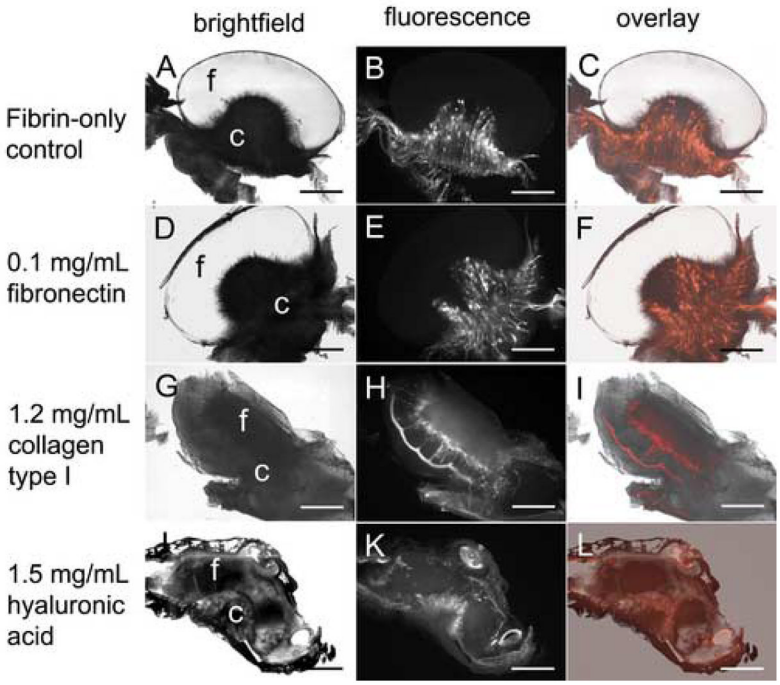

Figure 5. ECM additives within 10 mg/mL fibrin dramatically improve vascularization

10 mg/mL fibrin gels containing 10 ng/mL $VEGF_{165}$ (A–C) or $VEGF_{165}$ and 0.1 mg/mL human fibronectin (D–F), 1.2 mg/mL bovine collagen type I (G–I), or 1.5 mg/mL rooster comb hyaluronic acid (J–L) were placed on the CAM of 10 day old chick embryos. Three days post-placement on the CAM, embryos were intravitally injected with QDs and histologically processed as in Figure 1. Brightfield (A, D, G, J) and fluorescence (B, E, H, K) images were obtained using the M2BIO stereoscope. Fluorescence overlays (C, F, I, L) are shown for comparison of blood vessel and fibrin localization. In panels A, D, G, and J "f" and "c" indicate the location of the fibrin and CAM, respectively. Scale bars in all images are 200 μm.

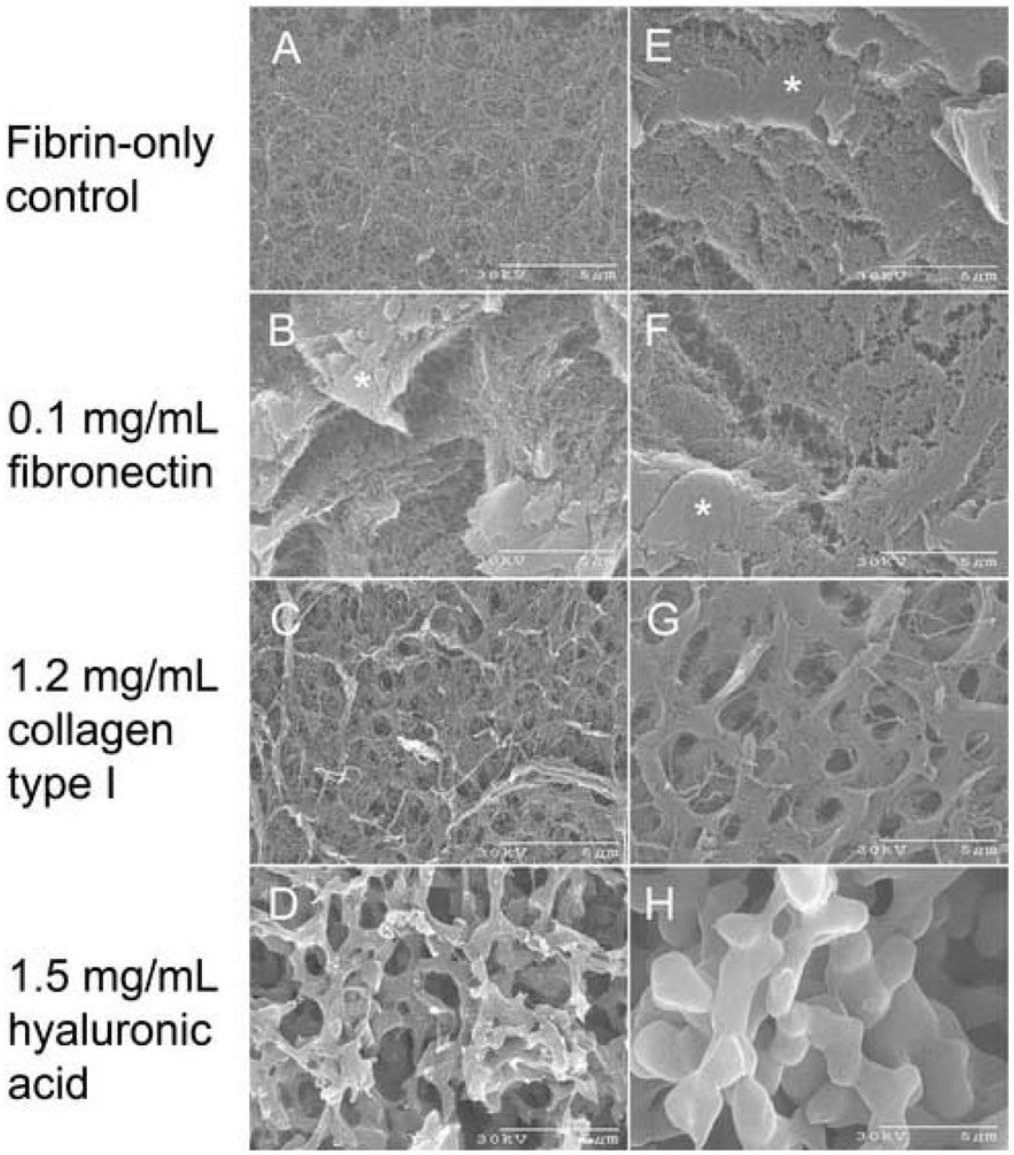

Figure 6. SEM analysis of fibrin scaffolds containing ECM additives

10 mg/mL (A–D) and 20 mg/mL (E–H) fibrin gels containing 10 ng/mL $VEGF_{165}$ and either no additive (A, E), 0.1 mg/mL fibronectin (B, F), 1.2 mg/mL collagen type I (C, G), or 1.5 mg/mL hyaluronic acid (D, H) were prepared for SEM analysis as described in the Materials and Methods. Cross-sectional cuts into the construct sometimes introduced artifacts as seen from the solid, plate-like surfaces in panels B, E, F (asterisks). Scale bars are shown at 5μm. Fiber diameter was measured and shown in Table 2.

Table 1

Semi-quantitation of CAM response to 10 mg/mL fibrin gels containing ECM additives in Figure 4[1]

Category	Fibrin-only control	0.1 mg/mL fibronectin	1.2 mg/mL collagen type I	1.5 mg/mL hyaluronic acid
Vessel penetration	1	1	2	3
Vessel density at construct interface	1	1	3	3
Overall CAM vessel density	4	4	2	1
Construct remodeling	1	1	3	4
Cellular invasion	-	1	3	N.D.

[1]Images from Figure 4 were analyzed and graded from lowest (1) to highest response (4). A dash (-) means that the response never occurred and N.D. means that the response could not be measured. Cellular invasion of fibrin containing 1.2 mg/mL collagen type I was determined by H&E analysis of the sample shown in Figure 4.

Table 2

Fiber thickness measurements of fibrin constructs in Figure 6[2]

				1.5 mg/mL hyaluronic acid	
	Fibrin-only control	**0.1 mg/mL fibronectin**	**1.2 mg/mL collagen type I**	**Struts**	**Fibers**
10 mg/mL fibrin construct	32 +/− 2	30 +/− 5	35 +/− 6	605 +/−96	31 +/− 5
20 mg/mL fibrin construct	32 +/−2	32 +/− 4	31 +/− 5	1725 +/− 187	30 +/− 6

[2]Reported data represents the mean diameter +/− the standard deviation of 10 random fibril measurements of the images shown in Figure 6 using Image J software (NIH, Bethesda, MD). Units for all fiber diameters are in nanometers.